Smart Structures and Systems, *Vol. 27, No. 6 (2021) 991-999*
DOI: https://doi.org/10.12989/sss.2021.27.6.991

Analytical model of shape memory alloy embedded smart beam, under actuated condition

Jagadeesh Veeraragu*, Yuvaraja Mani and Janakiraman M.

Department of Mechanical Engineering, PSG college of Technology, Peelamedu, Coimbatore, Tamilnadu-641004, India

(*Received June 16, 2020, Revised January 5, 2021, Accepted January 27, 2021*)

Abstract. Vibration characteristics of actuated Shape Memory Alloy (SMA) embedded smart composite beam are studied and it is extended to reduce the impact of resonance in cantilever beams. Smart composite beam with SMA embedded at neutral layer is studied for its vibrational characteristics under martensite and austenite conditions. The smart beam is developed as a analytical model incorporating the change in Young's modulus and damping factor under martensite and austenite conditions of SMA. The variation of natural frequency and damping are evaluated and verified with experimentation at different volume fraction of SMA. The thermo elastic nature of SMA and GFRP incorporated in the numerical model depicts the shift in natural frequency of 10% and reduction in magnification factor of 50% under actuation conditions. The frequency response of the smart beam depicts the capability of SMA in active vibration control and improvement of the structural health of composite beam. The thermo mechanical analytical model derived can be utilized to optimize the volume fraction of SMA to be embedded. The study can be extended to optimize actuation current to minimize the effect of resonance.

Keywords: structural health; smart beam; vibration control; actuation; analytical model; Shape Memory Alloy (SMA)

1. Introduction

The resonance of cantilever beam is strenuous problem to overcome. The potential of cantilever engineering structure is limited to counter the effect of resonance. Many structural implements have been made yet the resonance of the structure cannot be passively reduced. The functional range of many rotating cantilever beams such as wind turbines, propellers, etc. are limited due to its high amplitude vibration at resonance (Tang *et al*. 2015). The improvements on the vibrational characteristics through smart materials are extensive (Shu *et al*. 1997). Shape memory alloy (SMA) embedment is also provided evident results in reducing the vibrational amplitude of beams. The application of SMA to beams to improve vibrational characteristics are validated by many authors (Ni *et al*. 2007, Seelecke and Müller 2004). The martensitic and austenite conditions of the SMA have portrayed different characteristics and the same can be implemented to improve vibrational characteristics. The martensite state corresponding to passive control and austenite to active vibration control.

An active control to change the stiffness is required for flexible structure, which are achieved by actuating any of the smart materials like piezoelectric material shape memory alloy, magnetorheological fluid (Qiu 2014, Williams *et al*. 2005, Ma *et al*. 2016). Among these, shape memory alloy is receiving much attention as actuators for controlling the shape of the structures because SMA has a distinctive shape recovery effect which can generate significant forces during shrinkage as it undergoes its unique phase transformation by temperature change (Dönmez *et al*. 2010, Han 2005). Application of SMA has demonstrated their light weight and large force and displacement capabilities as well as low power consumption. Accordingly, this class of actuators provides exciting possibilities for miniaturization, simplicity and reliability (Lu *et al*. 2017, Vasundhara *et al*. 2019).

Experimental and theoretical investigation conducted by Khot *et al*. (2012) demonstrates the feasibility of utilizing Nitinol actuators, as a part of an active controller, to suppress the vibrations of a flexible beam. Dynamic characteristics of SMA reinforced at the neutral layer of the beam with different pre-strain conditions is studied with experimental and numerical model by Gupta *et al*. (2003) reveals that there is an extended upward shift in natural frequency with increase in pre-strain level. The simplified model experimental setup is explained in Fig. 1. Taking beams to equilibrium temperature, the composite beam is subjected to random vibrations and the resulting response is monitored by a micro-accelerometer bonded to the beam. The response is analysed in the frequency domain to determine the modes of vibration of the composite beam. The study concludes that SMA embedded flexible beams show high stiffness and are less susceptible to buckling. Modes of vibration of the activated Nitinol reinforced composite beams were found to be in the higher frequency bands relative to those of the un-activated or un-reinforced beams.

*Corresponding author, Ph.D. Student,
E-mail: Jagan047@gmail.com

ISSN: 1738-1584 (Print), 1738-1991 (Online)

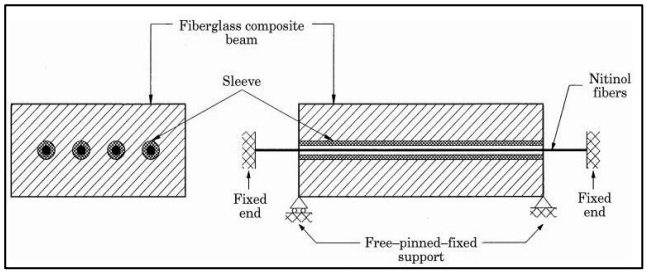

Fig. 1 Experimental setup of SMA embedded with different pre-strain value

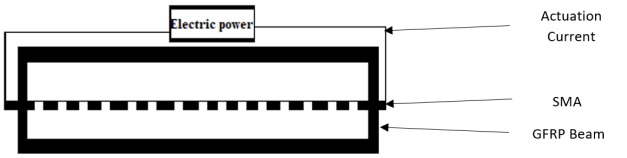

Fig. 2 Schematic representation of flexible beam with SMA activation

Jagadeesh *et al*. (2018) portrayed that the application of SMA in martensite condition significantly improves the vibration reduction of wind turbine blades up to 50%. Different volume fraction of SMA on the wind turbine blades are studied and the effect of SMA on reduction of vibrational amplitude improved with increase in volume of SMA embedded.

Yuvaraja and Kumar (2012) has conducted intensive study on vibration control of a flexible beam using SMA. The extent of vibration control is studied with tip displacement considering major influencing parameters such as diameter of SMA wire, amount input energy to activate SMA wire and number of actuators. Schematic representation of the flexible beam and SMA considered for experiment is shown in Fig. 2.

The experiment shows that the larger diameter wire significantly reduces the displacement for the same current rating and excitation frequency when compared to a wire of smaller diameter. SMA actuators provides vibration control over a wide range of excitation frequency and suitable for active vibration control.

Study on structural health monitoring of structures by Wang *et al*. (2017), Bayat *et al*. (2020), concludes the necessity of actuation and active vibration technique to reduce impact of vibratory forces on structures. In this study thermo-mechanical behavior of SMA wires will be used as actuation, to reduce impact of resonance of composite beams. The effect of SMA volume fraction in beams can be elaborated with an analytical model, incorporating the thermal behavior of the SMA under actuation.

2. Analytical model of cantilever smart beam

The cantilever composite beam is simplified as a lumped mass system and its analytical model is derived. The simplified model of the beam is shown in Fig. 3. The characteristic change in the properties of SMA embedded

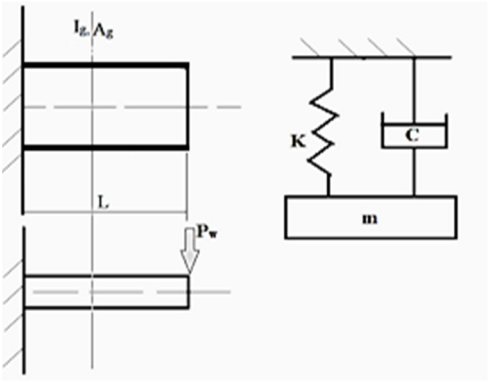

Fig. 3 Smart beams under cantilever condition

beam and variation in mechanical properties of beam are calculated using rules of mixture for composites.

The geometric parameters of the beam being

L = length of the beam
I = moment of inertia of beam at centre of gravity
A = Cross sectional area of beam at centre of gravity

Mani *et al*. (2020) calculated the natural frequency of cantilever continuous beam and simplified the beam as lumped mass system, which is equivalent to the study of single degree of freedom system with damping, governing equation is given by

$$m\ddot{x} + kx + c\dot{x} = 0 \tag{1}$$

The equivalent stiffness of cantilever beam Eq. (2) is applied in the above equation and considering the system to be undamped.

$$k = \frac{3EI}{L^3} \tag{2}$$

On simplifying the above equations (Wang *et al*. 2017a), the natural frequency Eq. (3) of the system is derived as

$$\omega^2 = \frac{3E_bI}{\rho_bAL^4} \tag{3}$$

Where E_b = Young's Modulus of the beam

I = mass moment of inertia
ρ_b = density of the beam
A = cross sectional of area of the beam

The properties in Eq. (3) holds good for analytical calculation of bending modes of simple beams made of GFRP. To incorporate the effect of SMA, beam's equivalent properties should be used. This can be achieved by using the rule of mixture composite.

Equivalent Young's Modulus (E)

$$\begin{aligned} E_b &= E_g + V_f(E_S - E_G) \\ E_b &= E_G + V_f(\Delta E) \end{aligned} \tag{4}$$

Equivalent density (ρ)

$$\rho_b = \rho_g + V_f(\rho_S - \rho_G)$$
$$\rho = \rho_G + V_f(\Delta\rho) \quad (5)$$

Incorporating the properties of SMA and GFRP together, the natural frequency of the composite cantilever beam can be written as

$$\omega^2 = \frac{3(E_g + V_f(\Delta E))I}{(\rho_g + V_f(\Delta\rho)))AL^4} \quad (6)$$

Eq. (6) relates natural frequency and volume fraction. The variation in the natural frequency of the beam can be visualized by dividing the natural frequency of the glass fiber beam, to obtain the non-dimensionalised shift in natural frequency.

The continuous beam can be simplified to forced vibration of a single degree of freedom system with damping, to obtain the harmonic response. The deflection equation is derived with dimensionless numbers, magnification factor and frequency ratio. A continuously varying force is simplified to a simple harmonic force of magnitude F_L.

$$m\ddot{x} + kx + c\dot{x} = F_L sin\omega t \quad (7)$$

The above differential equation should be solved to get the deflection of the system under harmonic excitation. Eq. (7) consists of complementary function and particular integral which should be solved to find the magnification factor for the system under excitation. The solved solution by considering a particular integral alone is expressed in terms of Magnification factor (μ) and frequency ratio (r).

$$\mu = \frac{1}{\sqrt{1 + \{r^2(r^2 + 2[2\zeta^2 - 1])\}}} \quad (8)$$

The magnification factor, obtained from Eq. (8), when multiplied with static deflection provides the actual deformation. The magnification factor of vibration is obtained as

Where $\zeta = damping\ ratio,\ r = \frac{\omega}{\omega_n},\ z_G = \frac{A_G}{I_G}$

$$\mu = \frac{3(E_G + V_f\Delta E)Z_G}{\sqrt{\omega^4 l^8 (\rho_G + V_f\Delta\rho)^2 + 3[3(E_G + V_f\Delta E)Z]\{3(E_G + V_f\Delta E)Z + 2\omega^2 l^4 (\rho_G + V_f\Delta\rho)(2\zeta^2 - 1)\}}} \quad (9)$$

The above equation evaluated with the damping ratio of the beam, under martensitic and austenitic conditions. Eq. (9) showcases the influence of damping and variation in material property of SMA under actuation current and the same can be visualised in Fig. 13.

3. Material characterization of SMA and epoxy-glass fibers

The variation of physical properties of SMA and epoxy-glass fibers based on temperature has to be characterized into an empirical relation, in order to evaluate the variation in natural frequency of smart beam. The relation between temperature and physical parameters will be incorporated into the analytical model, to study the behavior of SMA embedded composite beam. Thermomechanical behavior of SMA has been studied under different stresses by Ni *et al*. (2007), Lau (2002).

3.1 Characterisation of Thermo-mechanical beahaviour SMA

The shape memory alloy embedded inside a composite beam acts as a damper and a stiffening element, increasing the structural rigidity of the beam. The investigation on the SMA embedded composite beam under martensite and austenite conditions are limited. Nitinol wire of length 180 mm is considered for the characteristic's evaluation, similar to Bhargaw *et al*. (2013). An experimental setup has been made to extract the stress-strain relation of SMA under different actuation conditions. The SMA wires are actuated through electric current, which due to high resistance induces phase change in wires. The experimentation yields the variation of young's modulus across different actuation currents or martensite fraction.

The experiment is performed under martensite and austenite conditions of SMA, under pre-stress conditions of 12.5 MPa, 27.5 MPa and 37.5 Mpa. The mechanical properties such as strain, Young's modulus and temperature induced through actuation by current. The relation between Young's modulus and actuation current formed from the characterization of SMA.

3.2 Thermo-mechanical characteristics of Epoxy-glass fibre composite

The actuation of the smart material induces change in physical characteristics of polymer matrix composite (PMC), as the temperature of the smart beam increases. The behaviour of the smart beam under the variation of temperature can be inferred from the change in the physical parameters of the PMC. The study incorporated by Guo *et al*. (2013), provides with the numerical model of variation of flexural rigidity corresponding to the bending natural frequency of the smart beam. The empirical relation between the temperature and Young's modulus of glass fibre reinforced epoxy composite constitutes the behaviour of the smart beam under different temperature conditions. The GFRP becomes viscoelastic upon nearing the glass transition temperature, which induces reduction in tensile modulus of the structure. The variation in Young's modulus of fibre reinforced polymer with increase in temperature is modelled as

$$E(T) = E_0\left(1 - \frac{T - T_r}{T_{ref} - T_r}\right)^g \quad (10)$$

where modulus at room temperature is E_0, T_{ref} is the

temperature when modulus tends to zero, T_r-Reference temperature and g-power law index.

4. Evaluation of vibration characteristics under martensite and austenite conditions

With application of smart materials in structures by researchers such as Simonović *et al*. (2016), Lin *et al*. (1999), Lee *et al*. (2014), has experimentally showcased the vibration control using smart materials. Yet the influence of SMA on structures, under actuation has not been elaborated. In order to study the influence of SMA embedded wind turbine blade, a smart blade is developed, with 2 meters of 0.5 mm diameter SMA embedded inside. The volume fraction of SMA embedded inside the blade is 0.073% of volume of the composite wind turbine blade. The conventional and smart wind turbine blade are displayed in Fig. 4.

4.1 Smart composite beam

The vibration characteristics of the smart composite beam of different volume fractions are evaluated through experiment and the influence of volume fraction of SMA on the parameters are estimated. The smart composite beam is fabricated using hand layup technique, for different volume fractions.

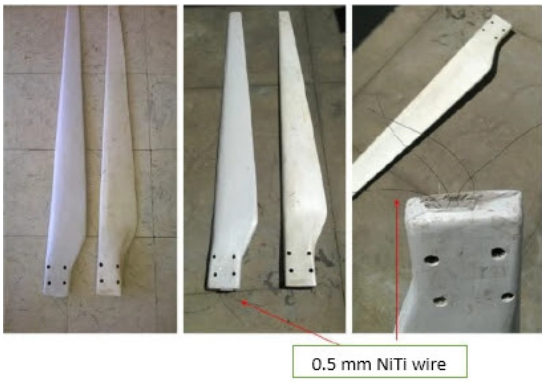

Fig. 4 Conventional and smart wind turbine blade

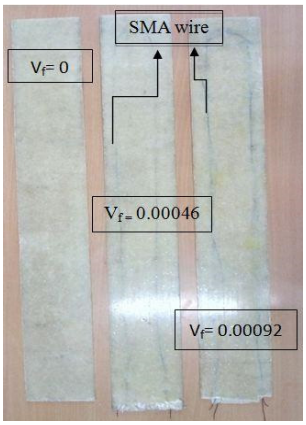

Fig. 5 Composite beam with different volume fraction of SMA

The effect of intrinsic properties of SMA, under martensitic and austenitic phase, on the dynamic parameters of smart composite beam are studied through modal analysis. The smart composite beams are fabricated using hand layup technique, using Epoxy-Glass fibers and SMA volume fraction of 0.042% and 0.092%. The volume fraction is kept too small, as to keep the change in physical properties of composite beams to a minimum. The smart composite beams thus produced are shown in Fig. 5.

4.2 Modal analysis of SMA embedded beam at martensitic and austenitic phase

The SMA embedded beam is evaluated for natural frequency and damping ratio under martensitic phase, in order to infer the influence of SMA on the damping and stiffness of the beam. The modal analysis is performed on the beam, at cantilever condition, by providing an impact pulse using an impact hammer. The time domain signal is collected using an accelerometer and then the signal is processed through a spectrum analyser, thus obtaining the frequency spectrum to identify the natural frequency of the beam. The schematic shown in Fig. 6 depicts the experimental setup for modal analysis.

The modal analysis thus performed on the composite beam, yielded the natural frequency to be 56 Hz. Similarly performing modal analysis on SMA embedded beam with different volume fraction of SMA, the variation of natural frequency and damping ratio with respect to volume fraction of SMA can be characterized.

The SMA wires induce 4% contraction through phase change, which is portrayed by Mouleeswaran *et al*. (2018).

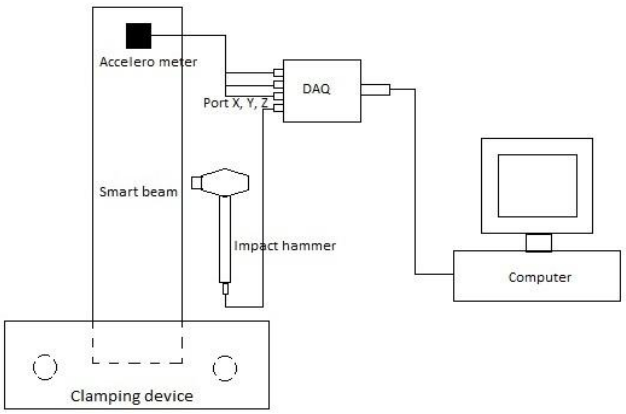

Fig. 6 Schematic diagram of modal analysis experimentation

Table 1 Natural frequency of smart beam under various volume fraction of SMA and actuation current

Volume fraction (%)	Frequency at different actuation current [Hz]				
	0 (A)	0.5 (A)	1 (A)	1.5 (A)	2 (A)
0	56.13	56.13	56.13	56.13	56.13
0.046	55.125	55.296	55.4667	54.784	53.76
0.092	54.933	55.333	55.667	54.667	53.333

Table 2 Damping ratio of smart beam under various volume fraction of SMA and actuation current

Volume fraction (%)	Damping ratio for different actuation current (ζ)				
	0 (A)	0.5 (A)	1 (A)	1.5 (A)	2 (A)
0			0.00969		
0.046	0.00998	0.01388	0.01226	0.01497	0.01931
0.092	0.01027	0.01388	0.01460	0.01780	0.02144

The SMA wires start its austenitic phase at 0.5A (at 45°C). The wires become completely austenitic at 2A (90°C). The variation in natural frequency and damping ratio of the smart composite beams estimated through modal analysis are tabulated in the Tables 1-2.

The damping ratio obtained from the modal analysis is used in Eq. (9) to obtain the magnification factor at resonance. The reduction in amplitude of vibration at resonance is studied to deduct the influence of the SMA under harmonic loading.

5. Results and discussion

The analytical equation Eq. (6) provides variation of natural frequency of the beam, under martensite conditions. The increase in volume fraction of SMA in the composite beam induces decrease in natural frequency. The decrease in the natural frequency of the beam, can be inferred to change in density being higher than the change in Young's modulus of the beam. The reduction of natural frequency with increase in volume fraction showcased in the analytical equation can be visualized in the Table 3. Table also relates the close proximity of the analytical results to experimental.

The effect of structural damping on the vibration response of the system has to be evaluated experimentally and incorporated in the analytical harmonic response of the beam, in order to study the influence of damping under martensitic and austenitic conditions of SMA. Similarly, Young's modulus of the SMA and GFRP beams are evaluated under increase in temperature, with respect to the actuation provided to the SMA wires.

The characteristics of the SMA wire are studied as per the experimental setup established and the physical parameters are evaluated for the actuation current provided to the wires. The corresponding actuation current excites the wire to respective temperature, due to high internal resistance provided by the wire to the current. Fig. 7 depicts the maximum temperature attained by the wire on actuation and time taken for the wires to reach respective temperature.

Table 3 Comparison of experimental and analytical non-dimensionalsied natural frequency of smart beam

V_f (%)	Experimental	Analytical
0.046	0.9821	0.9829
0.092	0.9787	0.9660

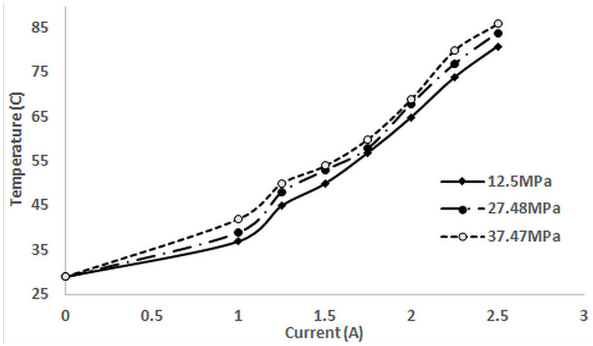

Fig. 7 Temperature of SMA under actuated conditions

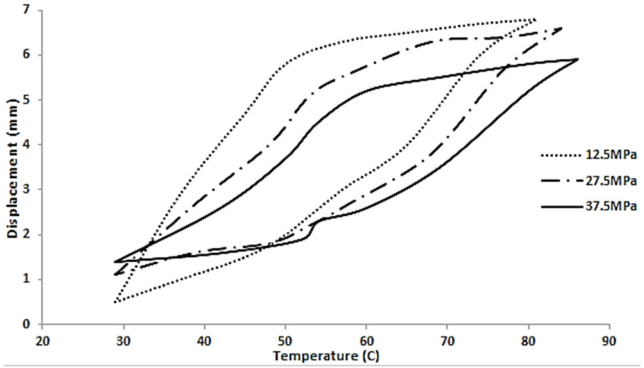

Fig. 8 Displacement vs temperature of SMA under actuation

The wires induce the 4% strain as per the shape memory effect on actuation and based on the different pre-stress provided to the wire, the respective strain is recorded. Fig. 8 depicts the displacement produced in the wire with actuation temperature. The pre-load provided to the wire causes change in displacement, which counters the compressive stress provided by the wire on actuation.

This change can be evaluated for calculation of Young's modulus of the SMA. The change in Young's modulus of SMA is evaluated from martensite to austenite conditions. The variation of Young's modulus of SMA based on the temperature of the wire, depicted in Table 4 and developed as an empirical relation. The same will be coupled in the analytical equation to study the effect of actuation of wire

Table 4 Variation of Young's modulus across actuation current

Temperature (°C)	Actuation current (A)	Young's Modulus (GPa)
30	0	15
42	1	23.08
50	1.25	28.75
54	1.5	33.42
60	1.75	37.46
69	2	41.28
80	2.25	44.9
86	2.5	48.46

under austenite conditions. The variation of SMA's Young modulus is presented in table and the respective empirical relation obtained from the regression curve fitting is portrayed in the Eq. (11).

The Young's modulus of SMA and actuation current provided are empirically related through regression equation. The Young's modulus of SMA, across actuation is expressed as

$$E_S(I) = \alpha\,(I)^2 + \beta\,(I) + E_A \qquad (11)$$

The coefficients of residuals α and β are 2.1849 and 8.3513 respectively. The Young's modulus of SMA at austenite start condition is E_A.

The analytical model developed for the smart beam under martensitic and austenite conditions are evaluated for different volume fractions of SMA. The evaluation portrays the variation of Young's modulus of SMA and GFRP with increase in volume fraction of SMA embedded and actuation current. The variation is portrayed in Figs. 9 and 10.

The experimentation performed on the smart composite beam, yields the vibration characteristics of the beam under different actuation conditions. The influence of SMA addition onto the composite beam, under martensitic condition, depicts decrease in the natural frequency of the smart composite beam with increase in volume fraction, at martensitic phase can be inferred from the Table 1. The reduction can be influenced by the difference in density being significantly larger than the difference in Young' s modulus of SMA and Epoxy-Glass fiber.

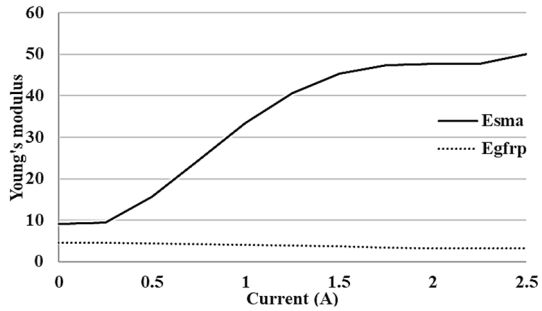

Fig. 9 Variation of Young's modulus of SMA and GFRP with actuation current

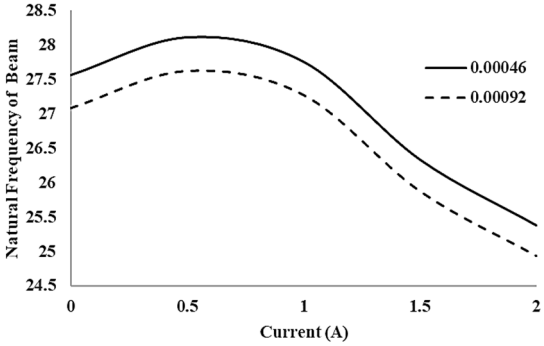

Fig. 10 Variation of natural frequency of smart beam under actuation current

The increase in damping ratio of the smart beam can be correlated to the increase in the super-elastic and shape memory effect of SMA under austenite conditions. The analytical model Eq. (9) is coupled with a correction factor, similar to Wieseman 1988, thus incorporating the non-linearity portrayed by the experimental result. The change in natural frequency of composite beam with embedment of SMA, characterized through experiment and analytical model Eq. (9) is portrayed in Fig. 13. The influence can be well characterized using non-dimensionalisation of natural frequency, with respect to the composite beam without SMA.

The similar evaluation of smart beam under austenite conditions, in Fig. 11, portrays the increase in Young's modulus of SMA, thus increasing the natural frequency of the beam. Lau (2002) validated the same for composite beams with clamped-clamped condition.

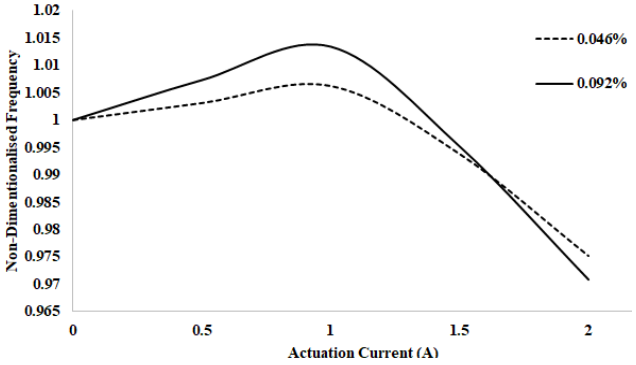

Fig. 11 Non dimensional frequency of smart beam across actuation current

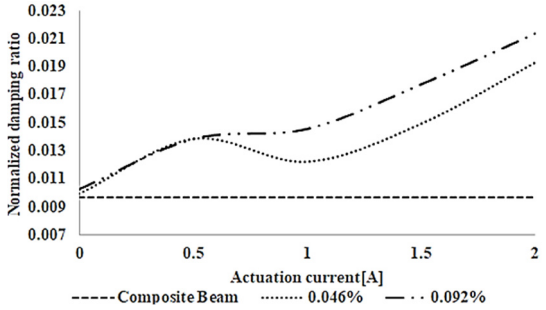

Fig. 12 Damping ratio of smart beam with actuation current, for various volume fraction

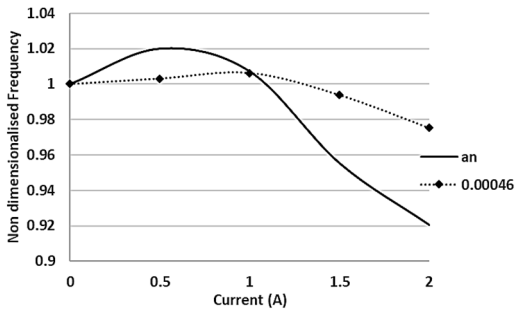

Fig. 13 Non dimensional frequency of smart beam across actuation current, experimental and analytical

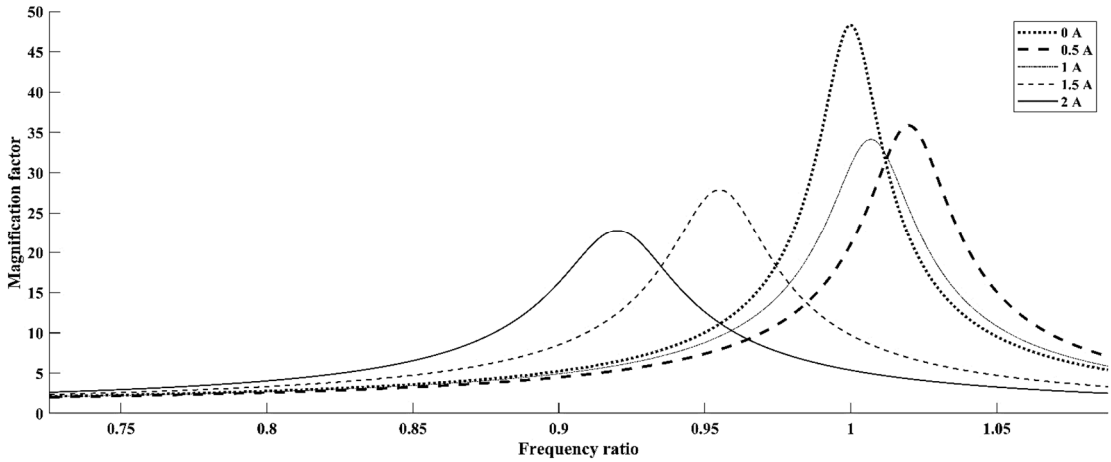

Fig. 14 Harmonic response of smart beam with actuation current

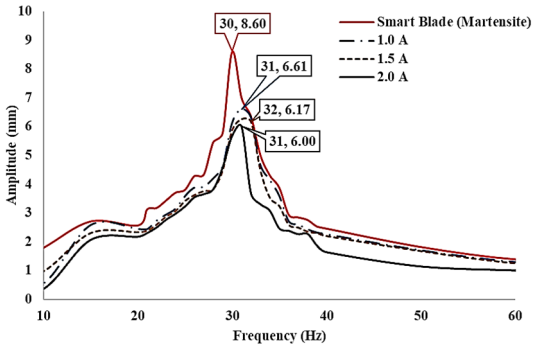

Fig. 15 Experimental harmonic response of smart blade under actuation current

As the smart composite beam's characteristics are evaluated under actuation current, the natural frequency of the beam increases. The internal compressive stress induced through actuation, causes stiffening of the beam, thus increasing the natural frequency of the beam. The actuation increased beyond 1A (60°C), the natural frequency of the smart beam decreased significantly. Fig. 11 depicts the decrease of the natural frequency beyond the actuation current of 1A.

It is observed that for increase in volume fraction there is continuous shift in frequency and improvement in damping, in Fig. 12. The displacement found to be decreased initially and for further increase of actuation current, a sharp increase is observed. This pattern continues for further increase of volume fraction.

The effect of increase in damping ratio can be inferred through the reduction in resonance. The magnification factor across the frequency ratio depicts the variation in frequency and amplitude of vibration at resonance. Using Eqs. (9)-(11) for various actuation currents are plotted in the Fig. 14. The response depicts that an increase in volume fraction of SMA reduces the amplitude of vibration at resonance. The magnification factor of vibration at resonance can be evaluated using the analytical model, under actuation conditions. The actuation of the smart beam induces an internal stress, which stiffens the beam. The increase in stiffness causes change in natural frequency of the beam. The super-elastic nature of SMA induces reduction of resonance amplitude.

Fig. 14 also depicts the change in natural frequency of the beam, under actuated conditions. The temperature of SMA increases with the increase in actuation current. The reduction in harmonic response of the system is associated with the improvement of damping along actuation current, with 0.046% volume fraction of SMA embedded on beam.

The reduction of resonance amplitude of the composite beam can be associated with vibration control and improvement in structural health of the composite beam.

The experimental harmonic response of a smart blade, embedded with 0.073% of SMA, under different actuation current is evaluated under base excitation of 1 g of acceleration. The smart blade, under martensite condition of SMA, displayed 8.6 mm of maximum amplitude of vibration under its natural frequency of 30 Hz. The effect of SMA under actuation current is portrayed in the Fig. 15, depicts the impact of SMA in the frequency response of the blade.

The experimentation depicts the similar increase and decrease in natural frequency of the blade under actuation current. The harmonic response of the smart blade showcases the improvement in the response amplitude of the structure under actuation current, which relates to the increase in damping of SMA wire under actuation current. Table 5 compares the reduction of resonance amplitude of the smart blade with the analytical model.

Table 5 Comparison of reduction in resonance amplitude between analytical model and experimentation

Actuation current	Analytical		Experimental	
	Magnitude	Reduction	Magnitude	Reduction
0 A	46	-	8.6	-
1 A	34	26%	6.61	23%
1.5 A	27	41%	6.17	28%
2 A	24	47%	6	30%

6. Conclusions

The smart composite beam embedded with SMA wires modelled analytically coupled with thermo mechanical behaviour of SMA and glass fibre depicts the thermal behaviour and vibrational characteristics of smart beam. The variation in Young's modulus with respect to actuation current and thus shift in natural frequency is depicted.

The change in modal characteristics with increase in volume fraction of SMA under martensitic condition portrays:

- Improvement of overall damping of the beam with increase in volume fraction of SMA, corresponds to the super elastic nature of SMA
- Reduction in natural frequency of the beam with increase in volume fraction is validated with the experimental model.

The actuation of the smart beam under experimental and analytical model depicts the similar variation in thermal behaviour of smart beam. The austenite state of SMA in the smart beam corresponds:

- With actuation current less than 1A, the natural frequency of the beam increases, corresponds to the improvement in the integrity of the beam.
- The harmonic response of the smart beam under actuation depicts the improvement of stiffness of the beam.
- With actuation more than 1A, the damping of the smart beam improves but natural frequency of beam reduces.
- The reduction in natural frequency is directly related to reduction of thermal behaviour of glass fibre at temperature above 60°C.

The harmonic response of smart beam under different actuation current depicts the effectiveness of active vibration control in smart beams. The deviation between the analytical and experimental response of the smart beam increases with actuation. The analytical model modified with Euler beam equation for thin beams, incorporated with the thermal equations Eq. (11) and damping model would improve analytical response. The analytical model of the smart beam can be improved with incorporation of martensitic, austenite starts and finish temperature models.

Acknowledgments

The authors would like to acknowledge Ministry of New and Renewable Energy (MNRE) India and PSG college of technology who have supported at various stages of this reported work.

References

Bayat, M., Pakar, I., Ahmadi, H.R., Cao, M. and Alavi, A.H. (2020), "Structural health monitoring through nonlinear frequency-based approaches for conservative vibratory systems", *Struct. Eng. Mech., Int. J.*, **73**(3), 331-337. https://doi.org/10.12989/sem.2020.73.3.331

Bhargaw, H.N., Ahmed, M. and Sinha, P. (2013), "Thermo-electric behaviour of NiTi shape memory alloy", *Transact. Nonferrous Metals Soc. China*, **23**(8), 2329-2335. https://doi.org/10.1016/S1003-6326(13)62737-5

Dönmez, B., Özkan, B. and Kadioğlu, F.S. (2010), "Precise position control using shape memory alloy wires", *Turk J. Electric. Eng. Comput. Sci.*, **18**(5), 899-912.

Guo, Z.S., Feng, J., Wang, H., Hu, H. and Zhang, J. (2013), "A new temperature-dependent modulus model of glass/epoxy composite at elevated temperatures", *J. Compos. Mater.*, **47**(26), 3303-3310. https://doi.org/10.1177/0021998312464080

Gupta, K., Sawhney, S., Jain, S.K. and Darpe, A.K. (2003), "Stiffness characteristics of fibre-reinforced composite shaft embedded with shape memory alloy wires", *Defence Sci. J.*, **53**(2), 167-173.

Han, Y.-L. (2005), "NiTi-wire shape memory alloy dampers to simultaneously damp tension, compression, and torsion", *J. Vib. Control*, **11**(8), 1067-1084. https://doi.org/10.1177/1077546305055773

Jagadeesh, V., Yuvaraja, M., Chandhru, A. and Viswanathan, P. (2018), "Investigations on Vibration Characteristics of Sma Embedded Horizontal Axis Wind Turbine Blade", *IOP Conference Series: Materials Science and Engineering*, Vol. 310, No. 1, p. 012067, Bengaluru, India, August. https://doi.org/10.1088/1757-899X/310/1/012067

Khot, S.M., Yelve, N.P., Tomar, R., Desai, S. and Vittal, S. (2012), "Active vibration control of cantilever beam by using PID based output feedback controller", *J. Vib. Control*, **18**(3), 366-372. https://doi.org/10.1177/1077546311406307

Lau, K.T. (2002), "Vibration characteristics of SMA composite beams with different boundary conditions", *Mater. Des.*, **23**(8), 741-749. https://doi.org/10.1016/S0261-3069(02)00069-9

Lau, K.T., Zhou, L.M. and Tao, X.M. (2002), "Control of natural frequencies of a clamped–clamped composite beam with embedded shape memory alloy wires", *Compos. Struct.*, **58**, 39-47. https://doi.org/10.1016/S0263-8223(02)00042-9

Lee, J.W., Han, J.H., Shin, H.K. and Bang, H.J. (2014), "Active load control of wind turbine blade section with trailing edge flap: Wind tunnel testing", *J. Intell. Mater. Syst. Struct.*, **25**(18), 2246-2255. https://doi.org/10.1177/1045389X14544143

Lin, Y.J., Lee, T., Choi, B. and Saravanos, D. (1999), "An application of smart-structure technology to rotor blade tip vibration control", *J. Vib. Control*, **5**(4), 639-658. https://doi.org/10.1177/107754639900500408

Lu, X., Li, G., Liu, L., Zhu, X. and Tu, S.T. (2017), "Effect of ambient temperature on compressibility and recovery of NiTi shape memory alloys as static seals", *Adv. Mech. Eng.*, **9**(2), 1-9. https://doi.org/10.1177/1687814017692287

Ma, Y., Wang, M., Yang, X., Zhang, D. and Hong, J. (2016), "Experimental investigation on the vibration tuning of a beam with shape memory alloy", *Proceedings of Turbo Expo: Power for Land, Sea, and Air*, August, pp. 1-7. https://doi.org/10.1115/GT2015-42262

Mani, Y., Veeraragu, J., Sangameshwar, S. and Rangaswamy, R. (2020), "Dynamic behavior of smart material embedded wind turbine blade under actuated condition", *Wind Struct., Int. J.*, **30**(2), 211-217. https://doi.org/10.12989/was.2020.30.2.211

Mouleeswaran, S.K., Mani, Y., Keerthivasan, P. and Veeraragu, J. (2018), "Vibration control of small horizontal axis wind turbine blade with shape memory alloy", *Smart Struct. Syst., Int. J.*, **21**(3), 257-262. https://doi.org/10.12989/sss.2018.21.3.257

Ni, Q.Q., Zhang, R.X., Natsuki, T. and Iwamoto, M. (2007), "Stiffness and vibration characteristics of SMA/ER3 composites with shape memory alloy short fibers", *Compos. Struct.*, **79**(4), 501-507. https://doi.org/10.1016/j.compstruct.2006.02.009

Qiu, Z.C. (2014), "Experiments on vibration suppression for a

piezoelectric flexible cantilever plate using nonlinear controllers", *J. Intell. Mater. Syst. Struct.*, **21**(2), 300-319. https://doi.org/10.1177/1077546313487762

Seelecke, S. and Müller, I. (2004), "Shape memory alloy actuators in smart structures: Modeling and simulation", *Appl. Mech. Rev.*, **57**(1), 23. https://doi.org/10.1115/1.1584064

Simonović, A.M., Jovanović, M.M., Lukić, N.S., Zorić, N.D., Stupar, S.N. and Ilić, S.S. (2016), "Experimental studies on active vibration control of smart plate using a modified PID controller with optimal orientation of piezoelectric actuator", *J. Vib. Control*, **22**(11), 2619-2631. https://doi.org/10.1177/1077546314549037

Shu, S.G., Lagoudas, D.C., Hughes, D. and Wen, J.T. (1997), "Modeling of a flexible beam actuated by shape memory alloy wires", *Smart Mater. Struct.*, **6**(3), 265. https://doi.org/10.1088/0964-1726/6/3/005

Tang, A.Y., Li, X.F., Wu, J.X. and Lee, K.Y. (2015), "Flapwise bending vibration of rotating tapered Rayleigh cantilever beams", *J. Constr. Steel Res.*, **112**, 1-9. https://doi.org/10.1016/j.jcsr.2015.04.010

Vasundhara, M.G., Senthilkumar, M. and Kalavathi, G.K. (2019), "A distributed parametric model of Brinson shape memory alloy based resonant frequency tunable cantilevered PZT energy harvester", *Int. J. Mech. Mater. Des.*, **15**(3), 555-568. https://doi.org/10.1007/s10999-018-9429-2

Wang, B., Wang, Z. and Zuo, X. (2017a), "Frequency equation of flexural vibrating cantilever beam considering the rotary inertial moment of an attached mass", *Mathe. Probl. Eng.* https://doi.org/10.1155/2017/1568019

Wang, Z., Qiao, P. and Shi, B. (2017b), "A comprehensive study on active Lamb wave-based damage identification for plate-type structures", *Smart Struct. Syst., Int. J.*, **20**(6), 759-767. https://doi.org/10.12989/sss.2017.20.6.759

Wieseman, C.D. (1988), *NASA Technical Memorandum Methodology For Matching Experimental And Computational Aerodynamic Data*, Langley Research Center.

Williams, K.A., Chiu, G.C. and Bernhard, R.J. (2005), "Dynamic modelling of a shape memory alloy adaptive tuned vibration absorber", *J. Sound Vib.*, **280**(1-2), 211-234. https://doi.org/10.1016/j.jsv.2003.12.040

Yuvaraja, M. and Kumar, M.S. (2012), "Experimental studies on SMA spring based dynamic vibration absorber for active vibration control", *Eur. J. Sci. Res.*, **77**(2), 240-251.

CC